Manuscript submitted to: Volume 2, Issue 2, 75-92.

AIMS Bioengineering DOI: 10.3934/bioeng.2015.2.75

Received date 18 April 2015, Accepted date 16 June 2015, Published date 18 June 2015

Research article

Altered Levels of Aroma and volatiles by Metabolic Engineering of Shikimate Pathway Genes in Tomato Fruits

Vered Tzin [1,3,*], Ilana Rogachev [1], Sagit Meir [1], Michal Moyal Ben Zvi [2,4], Tania Masci [2], Alexander Vainstein [2], Asaph Aharoni [1], and Gad Galili [1]

[1] Department of Plant Sciences, The Weizmann Institute of Science, PO Box 26, Rehovot 76100, Israel

[2] The Institute of Plant Sciences and Genetics in Agriculture, Faculty of Agricultural, The Hebrew University of Jerusalem, PO Box 12, Rehovot 76100, Israel

[3] The Boyce Thompson Institute for Plant Research, Ithaca, NY 14853, USA

[4] AB Seeds Ltd, PO Box 1 Misgav Ind. Area 2017900, Israel

* **Correspondence:** Email: vt223@cornell.edu; Tel: +607-216-8129; Fax: +607-254-1242.

Abstract: The tomato (*Solanum lycopersicum*) fruit is an excellent source of antioxidants, dietary fibers, minerals and vitamins and therefore has been referred to as a "functional food". Ripe tomato fruits produce a large number of specialized metabolites including volatile organic compounds. These volatiles serve as key components of the tomato fruit flavor, participate in plant pathogen and herbivore defense, and are used to attract seed dispersers. A major class of specialized metabolites is derived from the shikimate pathway followed by aromatic amino acid biosynthesis of phenylalanine, tyrosine and tryptophan. We attempted to modify tomato fruit flavor by overexpressing key regulatory genes in the shikimate pathway. Bacterial genes encoding feedback-insensitive variants of 3-Deoxy-D-Arabino-Heptulosonate 7-Phosphate Synthase (DAHPS; $AroG_{209\text{-}9}$) and bi-functional Chorismate Mutase/Prephenate Dehydratase (CM/PDT; $PheA_{12}$) were expressed under the control of a fruit-specific promoter. We crossed these transgenes to generate tomato plants expressing both the $AroG_{209}$ and $PheA_{12}$ genes. Overexpression of the $AroG_{209\text{-}9}$ gene had a dramatic effect on the overall metabolic profile of the fruit, including enhanced levels of multiple volatile and non-volatile metabolites. In contrast, the $PheA_{12}$ overexpression line exhibited minor metabolic effects compared to the wild type fruit. Co-expression of both the $AroG_{209\text{-}9}$ and $PheA_{12}$ genes in tomato resulted overall in a similar metabolic effect to that of expressing only the $AroG_{209\text{-}9}$ gene. However, the aroma ranking attributes of the tomato fruits from $PheA_{12}$//$AroG_{209\text{-}9}$ were unique and different from those of the lines expressing a single gene, suggesting a contribution of the $PheA_{12}$ gene to the overall metabolic profile. We suggest that expression of bacterial genes encoding

feedback-insensitive enzymes of the shikimate pathway in tomato fruits provides a useful metabolic engineering tool for the modification of fruits aroma and the generation of new combinations of tomato flavors.

Keywords: 3-Deoxy-D-Arabino-Heptulosonate 7-Phosphate Synthase; aromatic amino acids; metabolism; volatiles; Chorismate Mutase; Prephenate Dehydratase

Abbreviations

AAA = aromatic amino acids; VOCs = volatile organic compounds;
DAHPS = 3-deoxy-D-arabino-heptulosonate 7-phosphate synthase;
CM = chorismate mutase; PDT = prephenate dehydratase; FDR = false discovery rate.

1. Introduction

Tomato fruits are an important source of vitamins, dietary fibers, minerals, and antioxidants in the human diet [1]. During the ripening stage, tomatoes produce a large number of specialized metabolites, including volatile organic compounds [2,3], which serve as key components of the tomato fruit flavor [4,5]. These compounds are utilized to attract seed dispersers [6], as part of the plant defense mechanisms against herbivores [7] and in plant-plant communication. They are derived from a diverse set of precursors including amino acids, fatty acids and carotenoids [4]. The taste of a tomato is a result of the interactions of sugars, acids and a set of 20–30 volatile compounds. Among the several hundred volatile compounds accumulating in ripe tomato fruits, almost all of those related to flavor are derived from the essential amino acids phenylalanine (Phe), leucine (Leu) or isoleucine (Ile) [8]. It has also been proposed that volatile compounds produced in the ripe tomato fruits act as sensory cues for nutritional and health values [4,6].

One of the major biosynthetic pathways in plants is the shikimate pathway which leads to the synthesis of three aromatic amino acids (AAA) Phe, tyrosine (Tyr) and tryptophan (Trp) [9]. The shikimate pathway is a metabolic bridge between central carbon metabolism and specialized metabolism with regard to the regulation of AAA biosynthesis (Figure 1; [10,11]). In the last decade, many researches focused on exploring the enzymatic steps of the shikimate pathway, as well as the regulation of shikimate pathway enzymes. However, the carbon allocation towards the complex network of specialized metabolites that are derived from the AAA is not well understood [12,13]. One of the major regulatory mechanisms of flux through metabolic pathways is enzyme feedback inhibition loops, in which the end product metabolite of a given metabolic pathway feedback inhibits the activity of one of the enzymes of this pathway. Such enzyme feedback inhibition loops are common in metabolic pathways of amino acids [14], and are used to balance the metabolic homeostasis of the cell, to reduce toxicity and to promote plant development [15,16,17]. Plants containing modified, feedback-insensitive enzymes have been used to study the operation of metabolic pathways under uncontrolled conditions, and to produce plants tolerant to toxic combinations of amino acids or amino acid analogues, such as glyphosate (commercially known as Roundup; [18]). This also led to the identification of mutations in specific enzymes rendering them insensitive to feedback inhibition [14,17].

Overexpression of these feedback-insensitive genes allowed the plants to overcome the feedback inhibition of the native plant genes, "open" fluxes and change the carbon flow toward production of specialized metabolites. One such enzyme that was used encodes the first key enzyme of the shikimate pathway, namely, 3-Deoxy-D-Arabino-Heptulosonate 7-Phosphate Synthase (DAHPS; *E. coli* AroG) [19]. Another gene encodes a bi-functional Chorismate Mutase/Prephenate Dehydratase (CM/PDT; *E. coli* PheA), that converts chorismate via prephenate into phenylpyruvate (Figure 1, [20]). Previously, we overexpressed a bacterial gene encoding a mutant feedback-insensitive DHAPS ($AroG_{209}$) in *Arabidopsis thaliana* plants as well as in tomato fruits. In general, overexpression of the bacterial feedback-insensitive AroG increased the synthesis of all AAA, causing considerable enhancements in the levels of multiple specialized metabolites in both Arabidopsis and tomato [19,21]. In Arabidopsis vegetative tissues, constitutive expression of the bacterial $AroG_{209}$ caused massive metabolic changes and enhanced levels of phenylpropanoids, glucosinolates and phytohormones [19]. In tomato fruits, on the other hand, expression of $AroG_{209}$ under a fruit specific E8 promoter led to enhanced levels of multiple volatile and nonvolatile compounds derived from phenylpropanoids, in addition to volatiles and carotenoids derived from terpenoids. These results demonstrate the complex network between those metabolic pathways [21]. Furthermore, expression of the bacterial feedback-insensitive AroG in *Petunia × hybrida cv "Mitchell Diploid"* as well as expression of the endogenous PhDAHP1, resulted in dramatically increased levels of Phe and fragrant benzenoid-phenylpropanoid volatiles [12,22].

Phe is synthesized predominantly via the arogenate pathway [23], but the participation of the phenylpyruvate route in Phe biosynthesis has been previously suggested in Arabidopsis [24] and petunia [25]. The PheA gene converts chorismate via prephentate into phenylpyruvate. Previously, expression of a gene encoding a mutated *E.coli* feedback-insensitive PheA in Arabidopsis plants was shown to impact the synthesis of AAA and the specialized metabolites derived from them [24]. The PheA-expression lines had increased levels of specialized metabolites derived from Phe and Tyr, but reduced levels of specialized metabolites derived from Trp. These results imply regulatory cross-interactions between the flux of AAA biosynthesis from chorismate and their metabolism into various Phe specialized metabolites [24]. However, the possibility of using feedback-insensitive PheA in fragrant rich tissues such as tomato fruits or petunia petals has yet to be investigated. The significant variation between the specialized metabolites accumulating in Arabidopsis suggested that both feedback-insensitive AroG and PheA can function as excellent metabolic engineering tools for the production of specialized metabolites.

We aimed to study the metabolic pathways involved in determining the tomato fruit flavor. The ultimate goal of our research was to identify genes that control the synthesis of the flavor volatiles and use this knowledge to produce a better-tasting tomato. We hypothesize that manipulating the DAHPS and CM/PDT key enzymes will have different effects on the carbon flux and will allow identification of metabolites that are usually below detection level. Our previous studies suggested that massive metabolic changes occur in the $AroG_{209\text{-}9}$ transgenic tomatoes. Here we first tested the metabolic changes of tomato fruits expressing the PheA gene or both the $AroG_{209\text{-}9}$ and $PheA_{12}$ genes ($PheA_{12}$//$AroG_{209\text{-}9}$) crossed plants. We discovered that plants expressing both of the bacterial genes showed a unique metabolic profile that was predominantly impacted by expression of the $AroG_{209\text{-}9}$ gene, while the $PheA_{12}$ tomato line showed only minor metabolic differences. Our results suggest that this approach is suitable for altering tomato volatiles and aroma in a combinatorial manner.

Furthermore, this method can be used for the discovery of new metabolic networks by increasing the abundance of compounds that are usually below detection levels in the wild type fruit.

2. Materials and Methods

2.1. Plant material and growth condition

Flowers of greenhouse-grown tomato plants were marked at anthesis, and ripe red fruits were harvested approximately 48 days post anthesis. Each biological repeat was a mixture of 3–5 individual fruits. After harvesting, the peel and flesh (without the gel and seeds) were manually dissected and frozen in liquid nitrogen [26]. Homozygous plants of $AroG_{209\text{-}9}$ and $PheA_{12}$ were crossed and self-pollinated to generate the double transgenic cross line $PheA_{12}//AroG_{209\text{-}9}$ (F1 generation).

2.2. Plasmid construction and tomato stable transformation.

Genomic DNA was isolated from *Escherichia coli* (K-12 strain) and two genes, the 3-Deoxy-D-arabino-Heptulosonate 7-Phosphate Synthase isoform G (DAHPS; AroG) and the Chorismate Mutase/Prephenate Dehydratase (CM/PDT; PheA) were amplified and cloned as previously described [19,21,24]. The AroG and PheA genes were each fused to the tomato fruit-specific promoter E8 [27], whose expression is spatially and temporally regulated in mature tomato fruit [28]. The genes were fused at the 5'-end to a plastid targeting signal peptide originated from RUBISCO small subunit [29]. Primers are listed in Supplementary Table S1. Each of the chimeric genes was introduced into *Agrobacterium tumefacies* strain EHA-105 and used for plant transformation. Wild type tomato plants (M82 cultivar) were inoculated by submersing cotyledons in the transformed *A. tumefacies* culture as previously described [30,31]. Tomato transformation and genotyping were performed by Hazera Ltd (www.hazera.co.il/).

2.3. LC-MS Metabolomics analysis

Non-targeted metabolic analysis was performed using 500 mg of tomato peel and flesh, extracted in 80% methanol. Sample preparation and injection conditions were performed as previously described [32]. The analysis of the raw LC-MS (UPLC-qTOF-MS) data was performed using the XCMS software from the Bioconductor package (v. 2.1) for the R statistical language (v. 2.6.1) that performs chromatogram alignment, mass signal detection and peak integration [33]. XCMS was used with the following parameters: fwhm = 10.8, step = 0.05, steps = 4, mzdiff = 0.07, snthresh = 8, max = 1000. Injections of samples in the positive and negative ionization modes were performed in separate injection sets and pre-processing was done for each ionization mode independently. Differential mass ions were determined using a Student's *t*-test (JMP software) and 17 differential metabolites were subsequently assigned. Principal Component Analysis (PCA) plot and ANOVA tests were performed by the T-MEV4 software [34,35]. A Student's *t*-test analysis was performed on metabolites level using the JMP software (SAS).

2.4. Detection and profiling of volatile aroma compounds using GC-MS

GC-MS analysis of polar volatile compounds was carried out as previously described [21,36]. Briefly, a mix of 2–5 fruits (10 g) were harvested at the ripening stage (flesh and peel) and extracted with 30 ml MTBE:hexane (1:1) containing 2 μg isobutylbenzene as an internal standard. Following overnight incubation with shaking at 150 rpm, the extract was centrifuged at 10,500 g for 10 min and the supernatant was passed through a 0.2 μm filter. Samples were evaporated, using nitrogen, to a final volume of 200 μl before injection into a GC-MS instrument [19]. Identification of the compounds was based on a comparison of mass spectra and retention times with those of authentic standards (Sigma, Milwaukee, WI, USA) analyzed under similar conditions [21,37]. Statistical analysis was performed using the JMP software (SAS).

2.5. Sensory panel and evaluation of samples

A panel of 10 trained flavor specialists evaluated the aroma of samples by smelling the fruits as previously described [21]. Preliminary tests were carried out to improve the ability of the assessors to recognize odor changes and consistently quantify sensory properties. The panelists had been trained in the quantitative description of tomato attributes according to selection trials based on French norms (ISO8586-1, AFNOR V09-003). For each fruit sample, cut sections containing all fruit tissues were used for aroma evaluation by the panel. Values of individual fruits were ranked from zero (none) to 5 (very strong). The professional attributes considered were the following: acidic, floral, fresh, green, metallic musty, ripe, spicy, sweet and overall aroma intensity.

3. Results

3.1. Generating tomato fruits expressing feedback insensitive enzymes of the shikimate pathway

Our aim was to direct the central carbon metabolism through the shikimate pathway into specialized metabolites derived from the AAA. Therefore, our focus was on the first enzyme of the shikimate pathway, DAHPS, and the first and the second enzymes of Phe biosynthesis, CM/PDT. However, these enzymes are post translationally feedback regulated by their AAA products (Figure1). To overcome this regulation, we isolated, engineered and cloned two bacterial orthologues genes from *Escherichia coli*, and manipulated them to generate feedback insensitive isoforms of the genes. The *E. coli*, DAHPS gene, AroG, was point mutated in position 209. This mutation completely abolishes the Phe inhibition of the AroG allosteric site [38]. In the second enzyme, the *E. coli* bi-functional CM/PDT, PheA, the catalytic activities of the CM and PDT domains are located at amino acids 1–300 while the C-terminal domain is responsible for the allosteric feedback inhibition by Phe [39]. A truncated CM/PDT protein lacking the C terminus allosteric site retained the CM and PDT activities but did not exhibit feedback inhibition by Phe, and resulted in over accumulation of Phe [24,39]. A chimeric gene encoding the bacterial PheA under a tomato E8 fruit specific promoter was constructed and transformed into tomato plants. After selection of kanamycin resistant plants, the expression of the PheA gene in tomato fruit was verified by semi-quantitative RT-PCR (Figure S1). For each transgene, five independent transformation events were collected and subjected to LC-MS analysis, using both the negative and positive ion modes. This analysis revealed 5,723 and

7,125 mass signals, respectively. As shown in the PCA plots in Supplementary Figure S1, the most separated PheA transformation event was $PheA_{12}$ in both the negative and positive ion modes (Figure S2A and S2B respectively). As shown in Table S2, Phe level was significantly induced by more than two fold in $PheA_6$ and $PheA_{12}$ while Tyr and Trp were not changed. In addition, we selected unknown mass signals that were significantly altered mainly in $PheA_6$ and $PheA_{12}$ lines. Based on these results, the $PheA_{12}$ line was chosen for further work. As for the AroG gene, point mutation isoform 209, was fused to the E8 promoter and transformed in M82 tomato and transformation event number 9 was selected as previously characterized [21]. In order to detect the combined effect of the two shikimate pathway enzymes on tomato flavor, the $AroG_{209\text{-}9}$ and $PheA_{12}$ lines were crossed. $AroG_{209\text{-}9}$, $PheA_{12}$ and the cross $PheA_{12}$//$AroG_{209\text{-}9}$ line were analyzed and compared to the wild type (WT) M82 control.

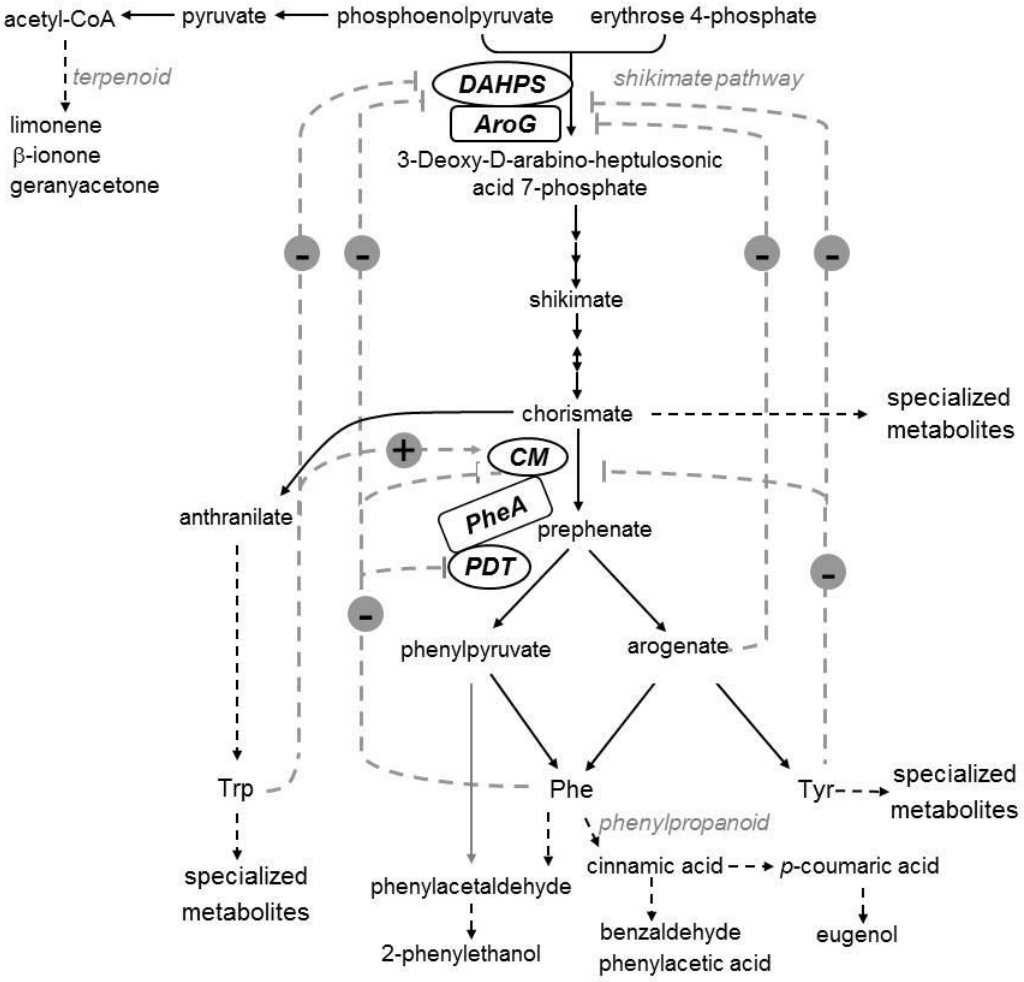

Figure 1. Scheme of the shikimate and AAA biosynthesis pathways in plants. Dashed gray lines represent post-transcriptional regulation of the DAHPS (bacterial AroG) and CM/PDT (bacterial PheA) by the AAA. Dashed black lines represent multiple enzymatic steps. Solid gray line represents biosynthetic pathway suggested by Kaminaga et al. 2006.

3.2. Effect of the AroG$_{209-9}$ and PheA$_{12}$ genes on the level of non-volatile metabolites in tomato fruit tissues

Fleshy tomato fruits develop in several marked stages, each possessing a characteristic metabolic profile [40]. Dramatic metabolic alteration of central metabolites occurs during fruit maturation [21,41] followed by induction of fruit flavor [4]. Therefore, we focused our study on ripe red tomato, which has the highest level of flavor volatiles. Fruits were separated into two tissues: (i) peel, which is typically composed of multiple cell types, including epidermis, collenchyma, and some parenchyma, and (ii) flesh, which refers to the pericarp material from which the peel has been removed and therefore is predominantly composed of parenchyma and collenchyma [32]. The transgenic tomato plants did not exhibit any morphological differences, and their course of development, including color breaking and ripening time was similar to that of the control plants (data not shown). Ripe fruits were harvested from AroG$_{209-9}$, PheA$_{12}$, PheA$_{12}$//AroG$_{209-9}$ and WT plants and analyzed by an established high-resolution LC-MS-based metabolomics platform (negative ion-mode; [42]). To get a global view on the metabolic effects, the LC-MS mass signals dataset was analyzed using PCA plots. As shown in Figure 2, the samples clustered into four groups: (i) flesh samples of the AroG$_{209-9}$ and PheA$_{12}$//AroG$_{209-9}$ lines; (ii) flesh samples of the PheA$_{12}$ and WT lines; (iii) peel samples of the AroG$_{209-9}$ and PheA$_{12}$//AroG$_{209-9}$ lines and, (iv) peel samples of the PheA$_{12}$ and WT lines. The AroG$_{209-9}$ and PheA$_{12}$//AroG$_{209-9}$ samples were closer to each other than to WT and PheA$_{12}$ but still did not overlap. This suggested that the major metabolic effects in the transgenic fruits are due to the presence or absence of the AroG$_{209}$ gene, while the PheA$_{12}$ gene has a minor contribution to the overall metabolic profile.

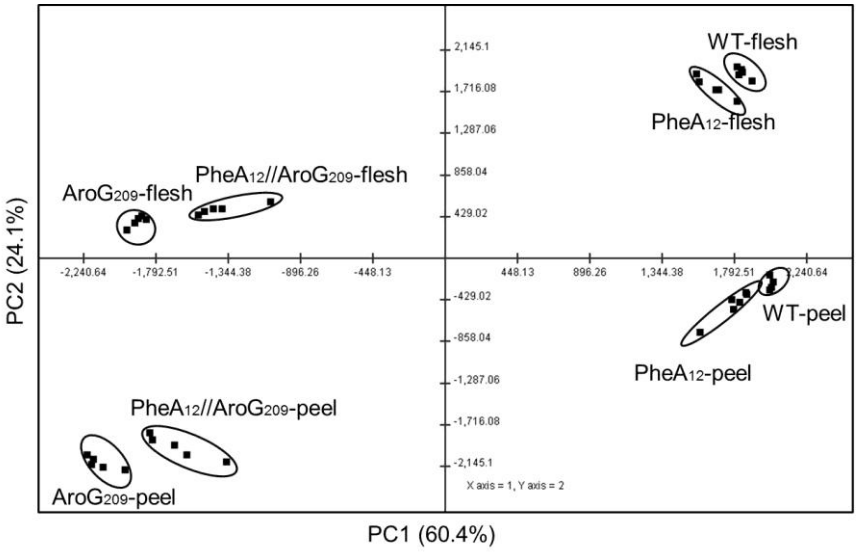

Figure 2. A PCA plot of LC-MS dataset obtained from the AroG$_{209-9}$ PheA$_{12}$ PheA$_{12}$//AroG$_{209-9}$, and wild type (WT) fruits. LC-MS analysis (negative ion mode) was performed on the peel and flesh tissues of the tomato red fruit (n = 5). PCA analysis was performed on the Log10 values of the mass signals (1,402) using the T-MEV4 software. Transgenic plants: PheA$_{12}$ (T3 generation) homozygote; AroG$_{209-9}$ (T2 generation) homozygote, and PheA$_{12}$//AroG$_{209-9}$ (F1 heterozygote).

To identify compounds whose levels differed between the transgenic lines, we compared the LC-MS mass signals to known chemical standards and libraries. As summarized in Table 1, 17 compounds were identified in the flesh and peel of the tomato fruits. In the flesh tissue (Table 1A), the levels of Phe and Tyr were increased in both $AroG_{209\text{-}9}$ and $PheA_{12}$//$AroG_{209\text{-}9}$ compared to the WT fruits. Trp level was increased only in the $AroG_{209\text{-}9}$ but not in the $PheA_{12}$//$AroG_{209\text{-}9}$ line. In addition, the level of isopropylmalic acid was increased in the flesh of both the $AroG_{209\text{-}9}$ and $PheA_{12}$//$AroG_{209\text{-}9}$ lines. The levels of caffeic acid-hexose and dicaffeoylquinic acid were significantly decreased in the flesh of both $AroG_{209\text{-}9}$ and $PheA_{12}$//$AroG_{209\text{-}9}$ transgene fruits.

Table 1. List of the metabolites identified by LC-MS in the peel (A) and flesh (B) of the $AroG_{209\text{-}9}$, Phe_{12}, $PheA_{12}$//$AroG_{209\text{-}9}$ and WT tomato fruits. Numbers in bold font indicate statistically significant differences between each of the lines compared to the WT (mean ± standard error) using multiple comparison Dunnett's test with WT as control.

A)	ES(-) m/z	Molecular Formula	Flesh-WT	Flesh-PheA	Flesh-AroG	Flesh- Cross, PheA12//AroG209-9
Name			Mean ±sterr	Mean ±sterr	Mean ±sterr	**Mean ±sterr**
Phenylalanine (S)	164.071	C9H11NO2	1.00 ±0.04	1.16 ±0.03	**7.68 ±0.35**	**5.39 ±0.19**
Tyrosine (S)	180.067	C9H11NO3	1.00 ±0.11	1.23 ±0.09	**23.26 ±0.87**	**9.54 ±0.93**
Tryptophan (S)	203.083	C11H12N2O2	1.00 ±0.07	1.16 ±0.06	**1.66 ±0.18**	1.38 ±0.14
2-Isopropylmalic acid (S)	175.061	C7H12O5	1.00 ±0.18	1.43 ±0.14	**3.80 ±0.40**	**4.62 ±1.39**
3-Caffeoylquinic acid (S)	353.087	C16H18O9	1.00 ±0.17	1.01 ±0.04	1.47 ±0.15	1.93 ±0.53
Acetoxyhydroxytomatine-FA	1152.539	(C52H85NO24)HCOOH	1.00 ±0.36	1.02 ±0.27	0.67 ±0.18	1.18 ±0.32
Caffeic acid-hexose	341.089	C15H18O9	1.00 ±0.08	1.21 ±0.11	**0.51 ±0.04**	**0.44 ±0.06**
Coumaric acid-hexose I	325.092	C15H18O8	1.00 ±0.17	0.91 ±0.18	0.85 ±0.12	0.90 ±0.11
Coumaric acid-hexose II	325.092	C15H18O8	1.00 ±0.22	1.09 ±0.19	1.03 ±0.16	1.22 ±0.22
Dicaffeoylquinic acid	515.119	C25H24O12	1.00 ±0.10	1.07 ±0.05	**0.61 ±0.11**	**0.61 ±0.13**
Ferulic acid-hexose	355.104	C16H20O9	1.00 ±0.20	1.09 ±0.18	0.39 ±0.09	1.14 ±0.60
Hydroxylated naringenin chalcone	287.057	C15H12O6	1.00 ±0.13	1.84 ±0.63	0.89 ±0.11	1.35 ±0.28
Hydroxylated naringenin-hexose (Eriodictyol-hexose)	449.108	C21H22O11	1.00 ±0.21	2.57 ±1.14	1.39 ±0.37	**4.08 ±1.12**
Naringenin chalcone-hexose	433.113	C21H22O10	1.00 ±0.20	1.17 ±0.33	**0.15 ±0.03**	0.43 ±0.12
Naringenin hexose	433.113	C21H22O10	1.00 ±0.12	1.48 ±0.63	2.45 ±0.61	**3.38 ±0.94**
Phloretin-di-C-hexose	597.1825	C27H34O15	1.00 ±0.14	1.00 ±0.13	**0.47 ±0.06**	0.69 ±0.12
Tricaffeoylquinic acid	677.152	C34H30O15	1.00 ±0.13	1.02 ±0.28	0.96 ±0.08	1.54 ±0.67

B)	**ES(-) Found m/z**	**Molecular Formula**	**Peel-WT**	**Peel-PheA**	**Peel-AroG**	**Peel- Cross, PheA12//AroG209-9**
Name			Mean ±sterr	Mean ±sterr	Mean ±sterr	Mean ±sterr
Phenylalanine (S)	164.071	C9H11NO2	1.00 ±0.10	1.57 ±0.11	**15.94 ±0.03**	**12.22 ±0.85**
Tyrosine (S)	180.067	C9H11NO3	1.00 ±0.12	1.45 ±0.31	**51.52 ±5.90**	**21.51 ±3.81**
Tryptophan (S)	203.083	C11H12N2O2	1.00 ±0.17	1.11 ±0.08	**2.37 ±0.09**	**1.68 ±0.10**
2-Isopropylmalic acid (S)	175.061	C7H12O5	1.00 ±0.11	0.82 ±0.12	**3.50 ±0.70**	**3.86 ±0.73**
3-Caffeoylquinic acid (S)	353.087	C16H18O9	1.00 ±0.14	0.81 ±0.04	**2.48 ±0.06**	1.71 ±0.45
Acetoxyhydroxytomatine-FA	1152.539	(C52H85NO24)HCOOH	1.00 ±0.13	0.96 ±0.07	0.46 ±0.15	0.52 ±0.26
Caffeic acid-hexose	341.089	C15H18O9	1.00 ±0.17	1.00 ±0.13	**0.81 ±0.10**	**0.57 ±0.12**
Coumaric acid-hexose I	325.092	C15H18O8	1.00 ±0.11	0.85 ±0.09	**9.21 ±1.79**	**5.61 ±0.88**
Coumaric acid-hexose II	325.092	C15H18O8	1.00 ±0.11	1.00 ±0.10	0.84 ±0.08	**0.57 ±0.04**
Dicaffeoylquinic acid	515.119	C25H24O12	1.00 ±0.10	1.28 ±0.09	**1.41 ±0.08**	1.00 ±0.07
Ferulic acid-hexose	355.104	C16H20O9	1.00 ±0.20	0.80 ±0.07	**0.22 ±0.06**	**0.21 ±0.05**
Hydroxylated naringenin chalcone	287.057	C15H12O6	1.00 ±0.09	1.08 ±0.09	**0.13 ±0.02**	**0.16 ±0.03**
Hydroxylated naringenin-hexose (Eriodictyol-hexose)	449.108	C21H22O11	1.00 ±0.10	1.42 ±0.13	1.46 ±0.37	3.10 ±1.14
Naringenin chalcone-hexose	433.113	C21H22O10	1.00 ±0.11	1.02 ±0.07	**0.34 ±0.04**	0.56 ±0.23
Naringenin hexose	433.113	C21H22O10	1.00 ±0.16	1.12 ±0.19	3.80 ±1.05	**10.01 ±4.73**
Phloretin-di-C-hexose	597.1825	C27H34O15	1.00 ±0.04	0.92 ±0.02	**0.34 ±0.06**	**0.50 ±0.07**
Tricaffeoylquinic acid	677.152	C34H30O15	1.00 ±0.12	1.13 ±0.10	**3.23 ±0.04**	**1.81 ±0.10**

The levels of naringenin chalcone-hexose and phloretin-di-C-hexose were significantly decreased in the $AroG_{209\text{-}9}$ while the levels of hydroxylated naringenin-hexose and naringenin hexose were significantly increased in $PheA_{12}$//$AroG_{209\text{-}9}$ only. None of the identified compounds were significantly changed in the flesh of the $PheA_{12}$ line relative to the WT.

In the peel tissue (Table 1B), the levels of all AAA, but most noticeably Phe and Tyr were increased in both the $AroG_{209\text{-}9}$ and the $PheA_{12}$//$AroG_{209\text{-}9}$ lines, as well as isopropylmalic acid, coumaric acid-hexose-I, and tricaffeoylquininc acid. The levels of caffeic acid-hexose, ferulic acid hexose and phloretin-di hexose were significantly decreased in both $AroG_{209\text{-}9}$ and $PheA_{12}$//$AroG_{209\text{-}9}$ lines. The levels of 3-caffeoylquinic acid, dicaffeoylquinic acid and naringenin chalcone-hexose were altered in the $AroG_{209\text{-}9}$ only. The level of naringenin hexose highly increased while coumaric acid hexose II deceased in $PheA_{12}$//$AroG_{209\text{-}9}$ only. Similarly to the flesh tissues (Table A1), none of the identified compounds were significantly changed in $PheA_{12}$ line. Interestingly, the induction of AAA in both flesh and peel was higher in the $AroG_{209\text{-}9}$ line compared to the $PheA_{12}$//$AroG_{209\text{-}9}$ line. In contrast, naringenin hexose levels were higher in the $PheA_{12}$//$AroG_{209\text{-}9}$ than in the $AroG_{209\text{-}9}$ line. These findings suggest that although no major changes were found in the level of the identified compounds in the $PheA_{12}$ line, its combined expression with $AroG_{209\text{-}9}$ in the $PheA_{12}$//$AroG_{209\text{-}9}$ line does affect the metabolic flux.

3.3. Effects of the expression of the AroG$_{209-9}$, the PheA$_{12}$ gene or both genes on volatile metabolites and fruit aroma

Our aim was to detect the changes in the level of volatile compounds in ripe red fruits expressing the AroG$_{209-9,}$ the PheA$_{12}$ gene or both genes. To that end, volatile metabolites accumulating in the tissue were extracted and analyzed by GC-MS as presented in Figure 3. The volatile compounds benzaldehyde, phenylacetaldehyde and phenylacetic acid were significantly increased in the AroG$_{209-9}$ and PheA$_{12}$//AroG$_{209-9}$ lines, compared to PheA$_{12}$ and WT. However, the level of phenylacetaldehyde was higher in the PheA$_{12}$//AroG$_{209-9}$ line than in the AroG$_{209-9}$ line. The levels of five other volatiles, eugenol (derived from *p*-coumaric acid; Figure 1), geranylacetone, β-ionone and limonene (derived from terpenoid) as well as benzaldehyde-4-methyl were reduced in the AroG$_{209-9}$ line, compared to the PheA$_{12}$ line and the WT. The PheA$_{12}$//AroG$_{209-9}$ line showed similar reduction of eugenol, geranylacetone, benzaldehyde-4-methyl and limonene, (derived from terpenoid) but no significant reduction in β-ionone and limonene compared to WT. Except for a slight increase in the eugenol and limonene levels, the PheA$_{12}$ tomato line showed no differences in the identified volatile compounds relative to the WT tomato fruits.

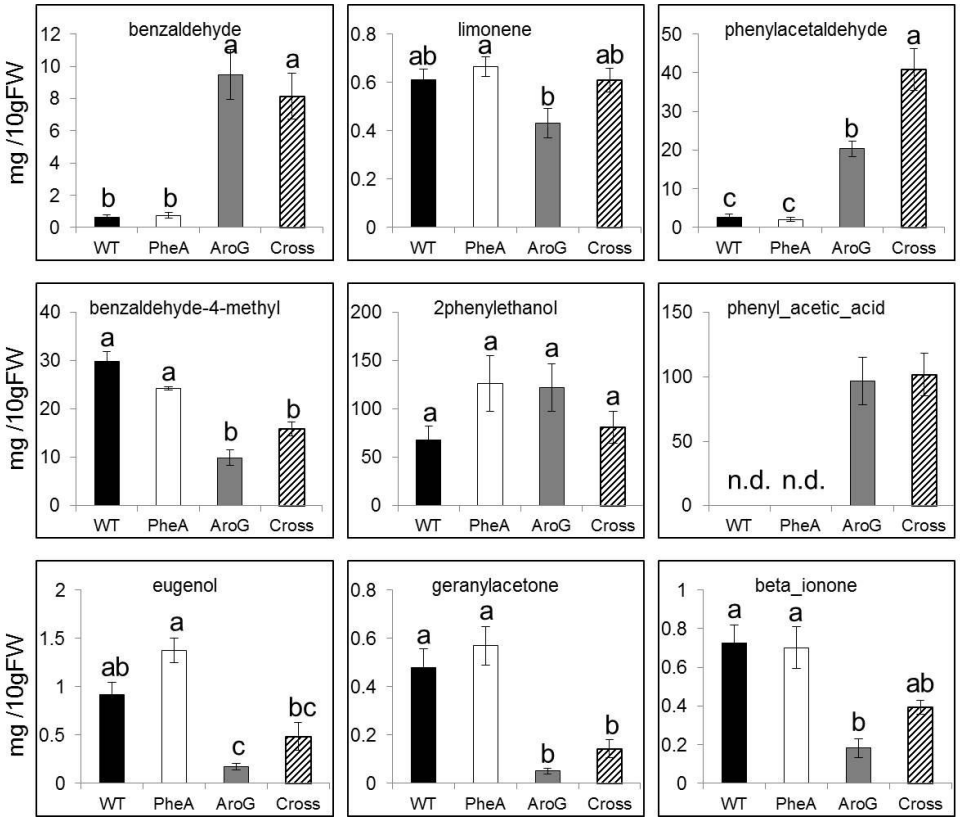

Figure 3. Internal pools of volatile compounds altered in red tomato fruits expressing the AroG$_{209-9}$ (AroG), PheA$_{12}$ (PheA) or both genes PheA$_{12}$//AroG$_{209-9}$ (Cross) line. Fruit samples were analyzed by GC-MS. Bars on top of the histograms indicate standard errors (n = 4). Letters indicate statistically significant differences between the three lines and WT using ANOVA all pairs comparison Tukey-Kramer HSD test. The AroG$_{209-9}$ data was previously published in Tzin et al. 2013.

Tomato aroma was also evaluated by a sensory panel. This test provides human insight into the flavor experience, where sensory attributes, preferences, and decisions can be statistically related to the chemical components in foods [43]. The organoleptic test was performed by a group of professionals trained in the quantitative description of tomatoes. Whole red fruits from each line were cut in half and evaluated by the various panel members by sniffing the samples (Figure 4). As shown in Figure 4, the panel suggested that the "acidic" aroma attribute was increased in the $PheA_{12}$//$AroG_{209\text{-}9}$ tomato fruits. The floral aroma attribute was increased only in the $AroG_{209\text{-}9}$ tomato as previously described [21], but not in the $PheA_{12}$ or $PheA_{12}$//$AroG_{209\text{-}9}$ fruits. In addition, it was suggested that the global aroma intensity of both $PheA_{12}$ and $PheA_{12}$//$AroG_{209\text{-}9}$ tomato fruits was decreased as compared to the $AroG_{209\text{-}9}$ tomato but not in comparison to the WT fruits. The other attributes were similar between the lines.

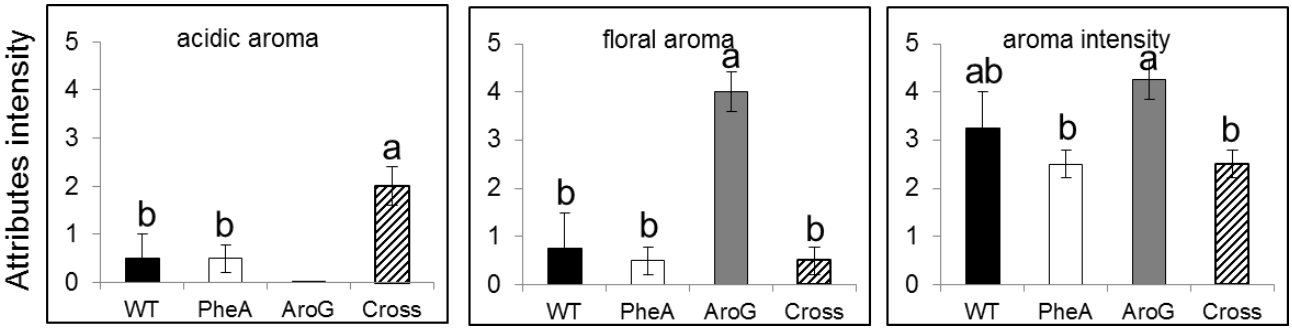

Figure 4. A sensory profile of red ripe tomatoes expressing the $AroG_{209\text{-}9}$ (AroG), $PheA_{12}$ (PheA) and both $PheA_{12}$//$AroG_{209\text{-}9}$ genes (Cross) line. Each attribute was scored on a scale between zero (none) to five (very strong). Bars on top of the histograms indicate standard errors (n = 4). Letters indicate statistically significant differences between the three lines and the WT using ANOVA all pairs comparison Tukey-Kramer HSD test. The $AroG_{209\text{-}9}$ data was previously published in Tzin et al. 2013.

4. Discussion

The results presented in this study suggest that overexpression of feedback insensitive mutants of $AroG_{209\text{-}9}$ //$PheA_{12}$ genes generated new tomato aroma composition (Figure 4). Previous research used ectopic expression of the petunia MYB transcription factor *ODORANT1* to alter the expression of a set of genes related to Phe metabolism in tomato fruits including *DAHPS*, *CM* and *Arogenate/Prephenate Dehydratase* [44]. This increased metabolic activity, was coupled to a considerably enhanced flux through part of the phenylpropanoid pathway, but did not result in induction of Phe-derived flavor volatiles, suggesting that factors beyond substrate availability limit their synthesis such as post-transcriptional regulation [44]. We chose a different approach using bacterial feedback-insensitive variants of biosynthetic enzymes in order to bypass enzyme feedback inhibition loops of the shikimate and AAA biosynthesis pathways (Figure 1). In general, the expression of these genes resulted in alteration in the production of several volatile as well as non-volatile compounds and in changes in fruit aroma. This emphasizes the importance of using ectopic expression of feedback-insensitive enzymes for metabolic engineering.

$PheA_{12}$, which is a feedback-insensitive isoform of the first and second enzymatic steps of the Phe biosynthesis, caused only minor metabolic changes in tomato (Figure 2–4 and Table 1). Although PCA analysis showed separation between $PheA_{12}$ and WT samples in either flesh or peel tissue (Figure 2), none of the identified compounds were differentially changed in this line (Table 1). This may be due to the small subset of metabolites that we were able to identify (17 non volatiles and 9 volatiles, see Table 1 and Figure 3, respectively). Volatile analysis suggested slight induction of eugenol and limonene compared to control plants, although the induction was not significant (Figure 4). Taken together, these results suggest that feedback-insensitive PheA does not play a major role in AAA metabolism and specialized metabolite derived from it in tomato fruits.

On the other hand, $AroG_{209\text{-}9}$, which is a feedback-insensitive form of the first enzymatic step of the shikimate pathway, caused massive metabolic changes in tomato (Figure 2–4 and Table 1). Similar results were previously shown in Arabidopsis vegetative tissues and petunia petals [12,21]. In order to enhance the carbon flux of AAA biosynthesis and direct it toward Phe derived volatiles, we crossed $PheA_{12}$ and $AroG_{209}$ tomato plants. The PCA plot separation showed close clustering of $AroG_{209\text{-}9}$ with the $PheA_{12}$//$AroG_{209\text{-}9}$ samples of peel and flesh tissue however, the PCA samples did not overlap in either tissue (Figure 2). Interestingly, several compounds had different levels in the $AroG_{209\text{-}9}$ fruits compared to the crossed tomato line (Figure 3 and Table 1). This implies that tomato fruits expressing both the $PheA_{12}$ and $AroG_{209\text{-}9}$ genes have a metabolic profile that is predominantly, but not solely, impacted by the expression of the $AroG_{209\text{-}9}$ gene.

Because volatiles are derived from a diverse set of precursors, including amino acids, fatty acids and carotenoids, changes in the level of these different precursors can impact tomato aroma. Phe and Tyr were significantly increased in the flesh of both the $AroG_{209\text{-}9}$ and $PheA_{12}$//$AroG_{209\text{-}9}$ lines, however the increase in their levels was higher in the $AroG_{209\text{-}9}$ line than in the cross line: Phe 7.68 and 5.39 and Tyr 23.2 and 9.34, fold changes respectively (Table 1A). This effect was also seen in the levels of AAA in the peel (Phe 15.94 and 12.22, Tyr 51.52 and 21.51 and Trp 2.37 and 1.68, fold changes respectively (Table 1B). The overall changes in Phe and Tyr are much more pronounced than in Trp in the peel and flesh of both the $AroG_{209\text{-}9}$ and the $PheA_{12}$//$AroG_{209\text{-}9}$ lines. As the levels of Phe and Tyr were higher in the $AroG_{209\text{-}9}$ line (Table 1), the effect on the aroma profile of the fruit might be different in these two lines, mainly due to Phe-derived volatiles (Figure 3–4). A Phe derived volatile compound, phenylacetaldehyde, was higher in the cross line than in the $AroG_{209\text{-}9}$ line (Figure 3). This may indicate additional regulatory metabolic steps of the Phe derived metabolites. In petunia, it's been demonstrated that phenylacetaldehyde is synthesized via Phe and phenylpyruvate [45]. Therefore, we suggest that in tomatoes the high induction of phenylacetaldehyde levels in the $PheA_{12}$//$AroG_{209\text{-}9}$ line might be due PheA contribution that drives Phe synthesis via phenylpyruvate (Figure 1). Carotenoids-derived precursor's β-ionone and geranylacetone [4] were reduced in both $AroG_{209\text{-}9}$ and $PheA_{12}$//$AroG_{209\text{-}9}$ lines (Figure 3) supporting cross-talk between phenylpropanoid and carotenoid (terpenoid) derived volatiles [46].

While several hundred volatiles have been identified in tomato, only a set of 20–30 volatile compounds actively contribute to tomato flavor; they are present in sufficient quantities to noticeably stimulate the olfactory system [4]. This threshold is determined by both the concentration of the substance and the organism's ability to detect it [47]. Flavor thresholds vary markedly between individuals and can be greatly influenced by the way in which the volatile is presented. The differences in volatile compounds between the lines (Figure 3) can give a varied tomato flavor (Figure 4).

5. Conclusion

This work demonstrates the potential for using feedback-insensitive enzymes to modify fruit flavor. Expression of feedback-insensitive enzymes in a combinatorial manner generates new aroma and affect flavor attributes. This approach is suitable for the enhancement of tomato volatiles and aromas as well as for the discovery of new metabolites and their biosynthesis and can be used in other plant species.

Acknowledgments

We would like to thank Meirav Gordon and Dr. Naomi Ben Dom from Hazera Ltd for tomato transformation and growth, and Natalie Dror from Frutarom Industries, Ltd. who organized the sensory panel and flavor evaluation of tomato samples. We thank Dr. Hadas Zehavi, Dr. Moran Oliva and Monica Franciscus for careful and critical reading of this manuscript. The research in Prof. Galili's lab was supported by grants from the Magnet Program of the Israeli Ministry of Industry, Trade and Labor and the Israeli Bio-TOV Consortium including Hazera Ltd., Evogene Ltd., Frutarom Ltd., Rahan Meristem (1998) Ltd. and Zeraim Gedera Ltd; The Bi-national Agriculture Research and Development (BARD) foundation; and AERI, the "Alternative Sustainable Energy Research Initiative" of the Weizmann Institute of Science. The research in Prof. Aharoni's laboratory was also supported by research grants from the European Research Council (ERC) project SAMIT (FP7 program), Sir Harry Djanogly, CBE, Mrs. Louise Gartner, Dallas, TX the Tom and Sondra Rykoff Family Foundation and Mr. and Mrs. Mordechai Segal, Israel. G. G. is an incumbent of the Bronfman Chair in Plant Sciences. A. A. is an incumbent of the Peter J. Cohn Professorial Chair.

Conflict of Interest

All authors disclose to have no conflict of interests.

References

1. Ioannidi E, Kalamaki MS, Engineer C, et al. (2009) Expression profiling of ascorbic acid-related genes during tomato fruit development and ripening and in response to stress conditions. *J Exp Bot* 60: 663–678.
2. Petro-Turza M (1987) Flavor of tomato and tomato products. *Food Rev Int* 2: 309–351.
3. Buttery R, Takeoka G, Teranishi R, et al. (1990) Tomato aroma components: identification of glycoside hydrolysis volatiles. *J Agr Food Chem* 38: 2050–2053.
4. Klee HJ, Giovannoni JJ (2011) Genetics and control of tomato fruit ripening and quality attributes. *Annu Rev Genet* 45: 41–59.
5. Zanor MI, Rambla JL, Chaib J, et al. (2009) Metabolic characterization of loci affecting sensory attributes in tomato allows an assessment of the influence of the levels of primary metabolites and volatile organic contents. *J Exp Bot* 60: 2139–2154.
6. Goff SA, Klee HJ (2006) Plant volatile compounds: sensory cues for health and nutritional value? *Science (New York, N Y)* 311: 815–819.

7. Dudareva N, Pichersky E, Gershenzon J (2004) Biochemistry of plant volatiles. *Plant Physiol* 135: 1893–1902.
8. Tikunov Y, Lommen A, De Vos R, et al. (2005) A novel approach for non targeted data analysis for metabolomics: large-scale profiling of tomato fruit volatiles. *Plant Physiology*: 1125–1137.
9. Vogt T (2010) Phenylpropanoid biosynthesis. *Mol Plant* 3: 2–20.
10. Tzin V, Galili G, Aharoni A (2012) Shikimate pathway and aromatic amino acid biosynthesis. *eLS ohn Wiley & Sons Ltd*.
11. Tzin V, Galili G (2010) New insights into the shikimate and aromatic amino acids biosynthesis pathways in plants. *Mol Plant* 3: 956–972.
12. Oliva M, Ovadia R, Perl A, et al. (2015) Enhanced formation of aromatic amino acids increases fragrance without affecting flower longevity or pigmentation in Petunia × hybrida. *Plant Biotechnology Journal* 13: 125–136.
13. Colquhoun TA, Clark DG (2011) Unraveling the regulation of floral fragrance biosynthesis. *Plant Signal Behav* 6: 378–381.
14. Pratelli R, Pilot G (2014) Regulation of amino acid metabolic enzymes and transporters in plants. *J Exp Bot* 65: 5535–5556.
15. Voll LM, Allaire EE, Fiene G, et al. (2004) The Arabidopsis phenylalanine insensitive growth mutant exhibits a deregulated amino acid metabolism. . *Plant Physiology* 136: 3058–3069.
16. Pratelli R, Voll LM, Horst RJ, et al. (2010) Stimulation of nonselective amino acid export by glutamine dumper proteins. *Plant Physiol* 152: 762–773.
17. Galili G, Amir R (2013) Fortifying plants with the essential amino acids lysine and methionine to improve nutritional quality. *Plant Biotechnol J* 11: 211–222.
18. Vivancos PD, Driscoll SP, Bulman CA, et al. (2011) Perturbations of amino Acid metabolism associated with glyphosate-dependent inhibition of shikimic Acid metabolism affect cellular redox homeostasis and alter the abundance of proteins involved in photosynthesis and photorespiration. *Plant Physiology* 157: 256–268.
19. Tzin V, Malitsky S, Ben Zvi MM, et al. (2012) Expression of a bacterial feedback-insensitive 3-deoxy-D-arabino-heptulosonate 7-phosphate synthase of the shikimate pathway in Arabidopsis elucidates potential metabolic bottlenecks between primary and secondary metabolism. *New Phytol* 194: 430–439.
20. Baldwin GS, Davidson BE (1981) A kinetic and structural comparison of chorismate mutase/prephenate dehydratase from mutant strains of Escherichia coli K 12 defective in the PheA gene. *Arch Biochem Biophys* 211: 66–75.
21. Tzin V, Rogachev I, Meir S, et al. (2013) Tomato fruits expressing a bacterial feedback-insensitive 3-deoxy-D-arabino-heptulosonate 7-phosphate synthase of the shikimate pathway possess enhanced levels of multiple specialized metabolites and upgraded aroma. *J Exp Bot* 64: 4441–4452.
22. Langer KM, Jones CR, Jaworski EA, et al. (2014) PhDAHP1 is required for floral volatile benzenoid/phenylpropanoid biosynthesis in Petunia × hybrida cv 'Mitchell Diploid'. *Phytochemistry* 103: 22–31.
23. Maeda H, Shasany AK, Schnepp J, et al. (2010) RNAi Suppression of Arogenate Dehydratase1 Reveals That Phenylalanine Is Synthesized Predominantly via the Arogenate Pathway in Petunia Petals. *Plant Cell* 22: 832–849.

24. Tzin V, Malitsky S, Aharoni A, et al. (2009) Expression of a bacterial bi-functional chorismate mutase/prephenate dehydratase modulates primary and secondary metabolism associated with aromatic amino acids in Arabidopsis. *Plant J* 60: 156–167.
25. Yoo H, Widhalm JR, Qian YC, et al. (2013) An alternative pathway contributes to phenylalanine biosynthesis in plants via a cytosolic tyrosine:phenylpyruvate aminotransferase. *Nature Communications* 4.
26. Adato A, Mandel T, Mintz-Oron S, et al. (2009) Fruit-surface flavonoid accumulation in tomato is controlled by a SlMYB12-regulated transcriptional network. *PLoS Genetics* 5: e1000777.
27. Deikman J, Kline R, Fischer RL (1992) Organization of Ripening and Ethylene Regulatory Regions in a Fruit-Specific Promoter from Tomato (Lycopersicon esculentum). *Plant Physiology* 100: 2013–2017.
28. Zhao L, Lu L, Zhang L, et al. (2009) Molecular evolution of the E8 promoter in tomato and some of its relative wild species. *J Biosciences* 34: 71–83.
29. Shaul O, Galili G (1993) Concerted regulation of lysine and threonine synthesis in tobacco plants expressing bacterial feedback-insensitive aspartate kinase and dihydrodipicolinate synthase. *Plant Molecular Biology* 23: 759–768.
30. McCormick S (1991) Transformation of tomato with *Agrobacterium tumefaciens*; Lindsey K, editor: Kluwer.
31. Filati J, Kiser J, Rose R, et al. (1987) Efficient transfer of a glyphosphate tolerance gene into tomato using a binary Agrobacterium tumefaciens vector. *Biotechnology* 5: 726–730.
32. Mintz-Oron S, Mandel T, Rogachev I, et al. (2008) Gene expression and metabolism in tomato fruit surface tissues. *Plant Physiology* 147: 823–851.
33. Smith CA, Want EJ, O'Maille G, et al. (2006) XCMS: processing mass spectrometry data for metabolite profiling using nonlinear peak alignment, matching, and identification. *Anal Chem* 78: 779–787.
34. Saeed AI, Sharov V, White J, et al. (2003) TM4: a free, open-source system for microarray data management and analysis. *Biotechniques* 34: 374–378.
35. Scholz M, Gatzek S, Sterling A, et al. (2004) Metabolite fingerprinting: detecting biological features by independent component analysis. *Bioinformatics* 20: 2447–2454.
36. Spitzer-Rimon B, Marhevka E, Barkai O, et al. (2010) EOBII, a Gene Encoding a Flower-Specific Regulator of Phenylpropanoid Volatiles' Biosynthesis in Petunia. *Plant Cell* 22: 1961–1976.
37. Davidovich-Rikanati R, Sitrit Y, Tadmor Y, et al. (2007) Enrichment of tomato flavor by diversion of the early plastidial terpenoid pathway. *Nat Biotechnol* 25: 899–901.
38. Hu C, Jiang P, Xu J, et al. (2003) Mutation analysis of the feedback inhibition site of phenylalanine-sensitive 3-deoxy-D-arabino-heptulosonate 7-phosphate synthase of Escherichia coli. *J Basic Microb* 43: 399–406.
39. Zhang S, Pohnert G, Kongsaeree P, et al. (1998) Chorismate mutase-prephenate dehydratase from Escherichia coli. Study of catalytic and regulatory domains using genetically engineered proteins. *J Biol Chem* 273: 6248–6253.
40. Carrari F, Baxter C, Usadel B, et al. (2006) Integrated analysis of metabolite and transcript levels reveals the metabolic shifts that underlie tomato fruit development and highlight regulatory aspects of metabolic network behavior. *Plant Physiology* 142: 1380–1396.

41. Osorio S, Vallarino JG, Szecowka M, et al. (2013) Alteration of the interconversion of pyruvate and malate in the plastid or cytosol of ripening tomato fruit invokes diverse consequences on sugar but similar effects on cellular organic acid, metabolism, and transitory starch accumulation. *Plant Physiol* 161: 628–643.
42. Rogachev I, Aharoni A (2012) UPLC-MS-based metabolite analysis in tomato. *Methods Mol Biol (Clifton, N J)* 860: 129–144.
43. Baldwin E, Scott J, Einstein M, et al. (1998) Relationship between sensory and instrumental analysis for tomato flavor. *J Am Soc Hortic Sci* 906–915.
44. Dal Cin V, Tieman DM, Tohge T, et al. (2011) Identification of Genes in the Phenylalanine Metabolic Pathway by Ectopic Expression of a MYB Transcription Factor in Tomato Fruit. *Plant Cell* 23: 2738–2753.
45. Kaminaga Y, Schnepp J, Peel G, et al. (2006) Plant phenylacetaldehyde synthase is a bifunctional homotetrameric enzyme that catalyzes phenylalanine decarboxylation and oxidation. *J Biol Chem* 281: 23357–23366.
46. Zvi MMB, Shklarman E, Masci T, et al. (2012) PAP1 transcription factor enhances production of phenylpropanoid and terpenoid scent compounds in rose flowers. *New Phytol* 195: 335–345.
47. Baldwin EA, Scott JW, Shewmaker CK, et al. (2000) Flavor trivia and tomato aroma: Biochemistry and possible mechanisms for control of important aroma components. *Hortscience* 35: 1013–1022.

Supplementary data

Table S1. Primers used in the research.

Gene name	Origin	Description	Purpose	Restriction site	Oligonucleotides
PheA	FW	PheA (from start codon)	Cloning	*HinD III ,SphI*	GCCAAGCTTATGGGCATGCCATCGGAAA ACCCGTTACTGGC
PheA	RV	PheA (no stop codon)	Cloning	*EcoRI*	CCCCGGAATTCCAACGTCGTTTTCGCCG GAACCTG
E8 tomato promoter	FW	E8 promoter	Cloning	*KpnI*	GGGGTACCTAGAAGGAATTTCACGAAA
E8 tomato promoter	RV	E8 promoter	Cloning	*SalI*	ACGCGTCGACCTTCTTTTGCACTGTGAA
PheA	FW	375bp product size	RT-PCR	-	CATGCCACTTGTCCAATTGTTG
PheA	RV	375bp product size	RT-PCR	-	GCCAGTAACGGGTTTTCCGATG
AroG	FW	700bp product size	RT-PCR	-	CATGCCACTTGTCCAATTGTTG
AroG	RV	700bp product size	RT-PCR	-	TCGTCGTTCTGATAATTCATCA

Table S2. List of the selected putative metabolites detected by LC -MS positive ion mode in five events of Phe transformation and WT tomato fruits. Numbers in bold font indicate statistically significant differences between each of the lines compared to WT (mean ± standard error) using Student t-test.

Putative Name	ES(+) Found m/z	RT (min)	M82 (n=7)	PheA1 (n=6)	PheA2 (n=6)	PheA3 (n=6)	PheA6 (n=4)	PheA12 (n=6)
Phe	165.896	2.14	1 ± 0.08	**1.45 ± 0.17**	**1.42 ± 0.11**	0.99 ± 0.12	**2.41 ± 0.40**	**2.04 ± 0.32**
Trp	205.099	3.87	1 ± 0.15	1.32 ± 0.12	0.82 ± 0.10	1.19 ± 0.17	1.14 ± 0.16	0.61 ± 0.12
Tyr	182.083	1.17	1 ± 0.19	1.10 ± 0.10	0.75 ± 0.11	1.18 ± 0.30	0.93 ± 0.13	0.78 ± 0.23
Acetoxy-dehydrotomatine	1090.547	17.19	1 ± 0.18	**0.38 ± 0.08**	**0.27 ± 0.07**	0.59 ± 0.20	0.41 ± 0.15	**0.48 ± 0.08**
Feruloyltyramine	314.140	15.35	1 ± 0.27	1.14 ± 0.25	0.43 ± 0.16	1.03 ± 0.23	0.95 ± 0.32	**0.24 ± 0.07**
Lycoperoside A/B/C (Acetoxytomatine) I	1092.563	17.75	1 ± 0.16	**0.32 ± 0.06**	**0.25 ± 0.07**	0.50 ± 0.19	**0.32 ± 0.12**	**0.44 ± 0.08**
N-Feruloylputrescine	265.155	4.04	1 ± 0.15	1.12 ± 0.11	1.27 ± 0.15	1.14 ± 0.10	1.07 ± 0.15	1.07 ± 0.10
M462T559	462.177	9.31	1 ± 0.31	**2.15 ± 0.30**	12.22 ± 2.85	0.64 ± 0.15	**11.12 ± 1.24**	**16.32 ± 2.38**
M674T1027	674.193	17.12	1 ± 0.31	1.47 ± 0.45	2.70 ± 0.80	0.28 ± 0.11	1.59 ± 0.20	**5.93 ± 0.52**
M251T192	251.141	3.20	1 ± 0.17	1.01 ± 0.30	1.09 ± 0.12	0.73 ± 0.23	1.29 ± 0.47	0.89 ± 0.18
M355T297	355.103	4.95	1 ± 0.13	**0.55 ± 0.07**	0.61 ± 0.16	**0.42 ± 0.08**	**0.48 ± 0.19**	0.86 ± 0.20
M550T129	550.160	2.14	1 ± 0.12	**3.84 ± 1.37**	**4.10 ± 0.66**	1.32 ± 0.38	**11.98 ± 2.44**	**8.85 ± 1.85**
M549T129	549.157	2.14	1 ± 0.08	**4.15 ± 1.13**	**4.08 ± 0.63**	1.31 ± 0.34	**9.29 ± 1.31**	**7.98 ± 1.34**
M852T308	852.313	5.13	1 ± 0.11	1.85 ± 0.59	**6.05 ± 1.19**	1.85 ± 0.92	**4.92 ± 1.94**	**3.85 ± 0.92**

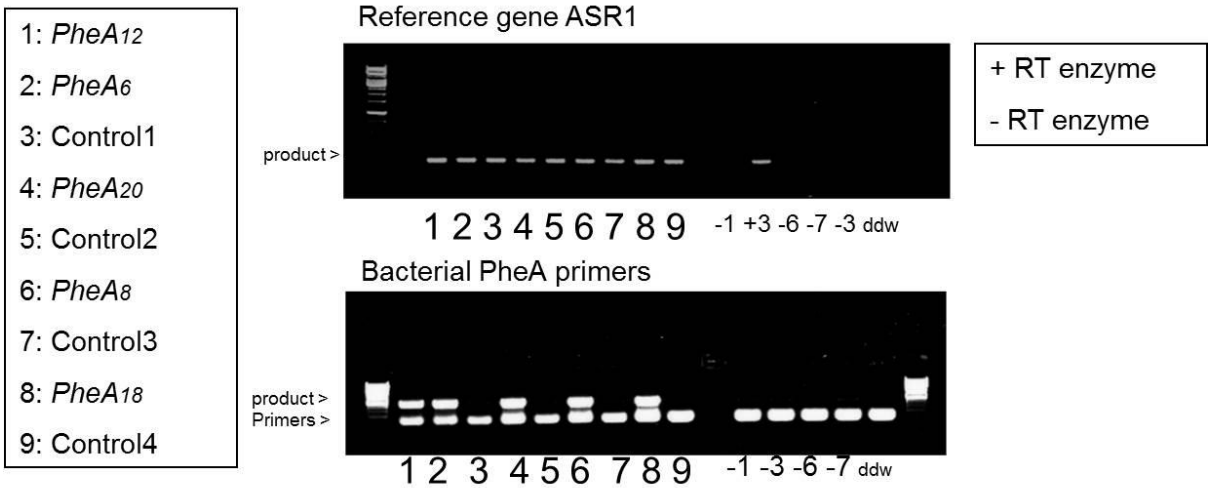

Figure S1. Semi-quantitative RT-PCR of PheA transformation events. Control, tomato fruits that were not transformed with the PheA gene. ASR1, Abscisic, Stress, Ripening gene used as positive control. RT, Reverse transcriptase.

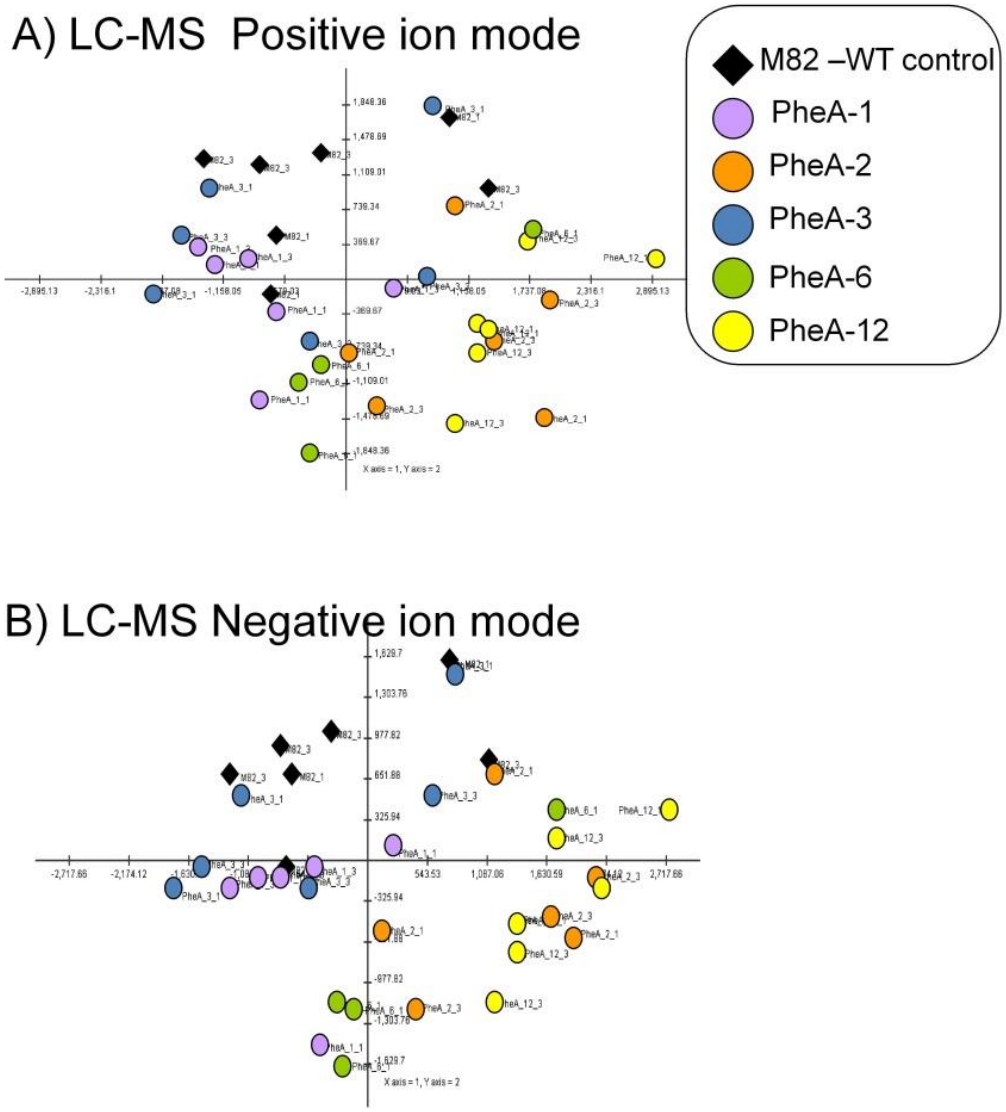

Figure S2: PCA plot of the five transformation events of *PheA* (T1) homozygous lines of tomato. Mass signals of chemical compounds were obtained by UPLC-QTOF-MS in the negative and positive ion modes (5,723 and 7,125 mass signals, respectively) from the tomato red fruit (n = 4–7; T1 generation). The PCA plot was done on the Log10 values and generated using the T-MEV4 software.